A sustainable reaction process for phase pure $LiFeSi_2O_6$ with goethite as an iron source

O. Skurikhina[a,b], M. Senna[c,*], M. Fabián[a], R. Witte[d], R. Tarasenko[e], V. Tkáč[e], M. Orendáč[e], M. Kaňuchová[f], V. Girman[e], M. Harničárová[g,h], J. Valíček[g,h], V. Šepelák[d,g], E. Tóthová[a,*]

[a] *Institute of Geotechnics, Slovak Academy of Sciences, Watsonova 45, 04001, Košice, Slovakia*
[b] *Faculty of Materials, Metallurgy and Recycling, Technical University of Košice, Letná 9, 04200, Košice, Slovakia*
[c] *Department of Applied Chemistry, Faculty of Science and Technology, Keio University 3-14-1 Hiyoshi, Kohokuku, 223-8522, Yokohama, Japan*
[d] *Institute of Nanotechnology, Karlsruhe Institute of Technology, Hermann-von-Helmholtz-Platz 1, 76344, Eggenstein-Leopoldshafen, Germany*
[e] *Institute of Physics, Faculty of Science, P.J. Šafárik University, Park Angelinum 9, 04154, Košice, Slovakia*
[f] *Faculty of Mining, Ecology, Process Control and Geotechnology, Technical University of Košice, Letná 9, 04200, Košice, Slovakia*
[g] *Faculty of Technology, Institute of Technology and Business in České Budějovice, 37001, České Budějovice, Czech Republic*
[h] *Technical Faculty, Slovak University of Agriculture in Nitra, 94976, Nitra, Slovakia*

Keywords:
$LiFeSi_2O_6$
Goethite
Reactivity of solid mixture
Mössbauer spectroscopy
Mechanochemistry

A B S T R A C T

Lithium-iron methasilicate ($LiFeSi_2O_6$, LFS), a member of clinopyroxene family, is an attractive compound for its multiferroic properties and applicability in energy-related devices. Conventional preparative method requires heating at elevated temperatures for long periods of time, with inevitable severe grain growth. We demonstrate that α-FeO(OH) (goethite) is superior as an iron source toward phase pure LFS over conventional hematite, α-Fe_2O_3. The exact phase purity, i.e., no trace of iron containing reactant, is confirmed in the goethite-derived LFS by ^{57}Fe Mössbauer spectroscopy. The grain growth of LFS during heating is suppressed to keep its crystallite size of 120 nm. Higher reactivity of goethite in comparison with hematite is mainly attributed to the dehydration of goethite, which in our case was accelerated by Li_2O. Related reaction mechanisms with the possible product pre-nucleation during mechanical activation are also mentioned. The magnetic properties of goethite-derived LFS are equivalent to those prepared via a laborious solid-state route. Thus, the presented preparative method offers a more sustainable route than conventional processing, and thus enables practical application of LFS.

1. Introduction

Lithium iron methasilicate, $LiFeSi_2O_6$ (LFS), belongs to the family of pyroxene with general chemical formula $M2M1T_2O_6$. Cations occu pying positions M2, M1 and T are coordinated in octahedral (for M2, M1) and tetrahedral (for T) layers [1], which are connected through their sidechains [2,3]. The crystal structure of pyroxene is either or thorhombic (*Pbca* and *Pbcn*) or monoclinic (*C*2/*c*, *P*2$_1$/*c*, and *P*2/*n*) [2]. The space group depends on the ionic radius of cationic species, tem perature and pressure of preparation [2]. M1 site can be occupied by di or trivalent cations (e.g., Fe^{2+}, Co^{2+}, Ni^{2+}, Al^{3+}, Cr^{3+}) in coordinated octahedra, while M2 with smaller ionic radii (e.g., Li^+, Na^+, Ca^{2+}, Mn^{2+}) forms distorted polyhedra with five to eight coordination number. The position T is occupied solely by a tetravalent Si or Ge ion. A new pyroxene, with T occupied by Ti^{3+}, was prepared by the authors' group for the first time via non conventional one step mechanochemical synthesis [4].

Potential application of pyroxenes depends mostly on their chemical composition [5]. In the case of $LiFeSi_2O_6$, magnetic properties and crystal structure were extensively studied [6 9]. LFS crystallizes in a monoclinic crystal structure and structural phase transition from *C*2/*c* to *P*2$_1$/*c* occurs at 230 K or 0.8 GPa [5], with simultaneous change in its ferroelectricity [10]. It was found that this material exhibits anti ferromagnetic (AF) ordering with T_N = 19.5 K and θp = −33 K [6]. In the magnetic crystal structure, intrachain ferromagnetic coupling oc curs between Fe Fe, and interchain antiferromagnetic coupling be tween chains of Fe cations [6]. Moreover, electrochemical properties of this type of pyroxene were studied, regarding further application as electrode materials for Li ion batteries [11,12].

Conventional ceramic preparative methods of LFS are laborious, with prolonged heating time and repeated sintering [13,14], or pre liminary hydrothermal processes [11,12]. It is recognized that

* Corresponding authors.
E-mail addresses: senna@applc.keio.ac.jp (M. Senna), etothova@saske.sk (E. Tóthová).

preliminary mechanical activation of the starting mixture enables decrease of heating temperature and crystallite size [15]. We had been previously challenged to prepare nanocrystalline LFS by a combined mechano/thermal process, starting from a mixture comprising hematite, Li_2SiO_3, and SiO_2 [9], while nano glassy material was obtained solely by a prolonged milling [9]. However, a trace of Fe precursor (hematite) had persisted, which significantly affects the magnetic properties of the product. Elimination of hematite was not possible as far as we started from hematite as an iron source.

Therefore, we challenged to obtain phase pure LFS with another iron source. We focused on α FeO(OH) (goethite), which is a good precursor of magnetic ferric oxides, i.e., maghemite and magnetite [16], due to its high reactivity. We compared the reaction process and properties of the products obtained from goethite with those from hematite. Additionally, we tried to replace a purchased intermediate, Li_2SiO_3, used in our previous study, with cheaper and hence more affordable Li_2O and SiO_2.

2. Experimental

2.1. Preparation

In the first step, two different stoichiometric mixtures composed of Li_2O (Merck, 97%, d_{50} = 25 μm), SiO_2 (Merck, purum p.a., d_{50} = 26 μm) and an iron source, either hematite, α Fe_2O_3 (Merck, ≥96%, d_{50} = 0.55 μm) or goethite, α FeO(OH) (kindly donated by Toda Kogyo, Otake, Japan, d_{50} = 11 μm) were used. Each mixture, expressed by Equations (1) and (2) in a total amount of 4 g, was milled in a planetary ball mill, Pulverisette 7 premium line (Fritsch) for 60 min at 600 rpm in air atmosphere. A milling bowl (80 cm^3 in volume) and balls (18 pcs, 10 mm in diameter) made of tungsten carbide were used. The ball to powder weight ratio was 33:1.

$$Li_2O\ (s) + \alpha\ Fe_2O_3\ (s) + 4SiO_2\ (s) \rightarrow 2LiFeSi_2O_6\ (s) \quad (1)$$

$$Li_2O\ (s) + 2\alpha\ FeO(OH)\ (s) + 4SiO_2\ (s) \rightarrow 2LiFeSi_2O_6\ (s) + H_2O\ (l) \quad (2)$$

In the second step, the mechanically activated mixtures were subsequently heated up to 1000 °C, held for 60 min, and then cooled down to room temperature in air.

2.2. Characterization

X ray diffraction (XRD) analysis was performed using a D8 Advance diffractometer (Brucker) with the CuKα radiation in the Bragg Brentano configuration. The generator was set up at 40 kV and 40 mA. The divergence and receiving slits were 0.3° and 0.1 mm, respectively. The XRD patterns were recorded in the range of 2θ = 10 80° with a step of 0.04°. Rietveld refinement was performed in the space group C2/c, using Fullprof computer program [17]. The XRD line broadening was evaluated by the refinement of regular Thompson Cox Hastings pseudo Voigt function parameters. In order to obtain proper geometry set up and to eliminate instrumental broadening, the latter was determined by refinement of LaB_6 standard specimen. The JCPDS PDF database was utilized for phase identification [18].

^{57}Fe Mössbauer measurements were carried out in a transmission mode at room temperature. As a source of the γ ray, ^{57}Co in Rh matrix was used. The velocity scale and isomer shifts were calibrated using a metallic α Fe foil absorber. The Mössbauer data were fitted using the *WinNormos* software package (Wissel Company, R. A. Brand).

Temperature dependence of static magnetic susceptibility was measured on a powder sample using a commercial Quantum Design SQUID magnetometer. The magnetic susceptibility was measured in the temperature range from 2 K to 400 K at 1 T. Diamagnetic contribution to magnetic susceptibility was subtracted using Pascal constants.

Electronic properties were examined by X ray photoelectron spectroscopy with SPECS instrument equipped with PHOIBOS 100 SCD. Non monochromatic X ray source was used at the transition energy 40 eV and the core spectra at 50 eV, at room temperature. All spectra were acquired at a basic pressure of 2×10^{-8} mbar with Mg Kα excitation at 10 kV (150 W). The data were analyzed by SpecsLab2 CasaXPS software (Casa Software Ltd.). A Shirley and Tougaard type baseline were used for all peak fits. The spectrometer was calibrated against Ag 3d. All samples showed variable degrees of charging due to their insulating nature, which was resolved by the calibration based on the C1s binding energy.

Fourier transform infrared (FT IR) in transmission mode was performed using a Tensor 27 spectrometer (Bruker). The samples were prepared by a KBr pellet method and measured in the frequency range of 4000 400 cm^{-1} with a resolution of 2 cm^{-1}, by repeating 64 scans. KBr was dried before the analysis at 100 °C for 1 h. The spectra were expressed as absorbance versus wavenumber (cm^{-1}).

Microstructure of the product was examined by a high resolution scanning transmission electron microscope (S)TEM, JEOL 2100F, with a Schottky field emission gun and working at an acceleration voltage of 200 kV. The powder sample was crushed in a mortar, stirred in ethanol and ultrasonicated for 8 min at varying frequencies to disperse particles. Subsequently, a drop of 1.5 μm volume was fixed on a copper supported grid covered with thin carbon film. Then it was immediately placed under a vacuum of 10^{-2} Pa in order to ensure consistent evaporation of ethanol.

Thermogravimetric measurements were carried out using STA 449 Jupiter thermal analyzer (Netzsch). The measurements were performed at steady air flow from 30 °C up to 1000 °C, with a heating rate of 10 °C/min.

3. Results and discussion

3.1. Consequences of mechanical activation

Fig. 1 shows the XRD patterns of two stoichiometric mixtures composed of Li_2O, SiO_2 and two Fe sources, i.e., hematite (α Fe_2O_3) or goethite (α FeO(OH)), from the top to the bottom: mechanically activated mixtures and thermally treated mechanically activated mixtures. The XRD profiles of the starting mixtures (not shown) are characterized by the sharp diffraction peaks corresponding to the reactants: Li_2O (JCPDS Card No. 73 0593), SiO_2, quartz, (JCPDS Card No. 01 0649) and Fe sources, α Fe_2O_3 (JCPDS Card No. 72 0469) or α FeO(OH) (JCPDS Card No. 81 0463), respectively. The XRD patterns of the used Fe sources are presented in supplementary material, Fig. S1. Annealing to 1000 °C of both mixtures without preliminary mechanical activation (not shown) led to the formation of LFS only in a small amount. The intensity of LFS diffraction peaks were higher from hematite as an iron source, which indicates a greater amount of product was synthesized compared to the case with goethite. Among the diffraction peaks of the reactant, those of quartz were predominant, when goethite was used. Mechanical activation led to entirely different phase composition. A small peak of quartz at 2θ ~26.6° persisted just after milling. However, no peaks of iron precursor were observed when goethite was used. When hematite was used, small peaks of the iron reactant were still observed. After subsequent heating, we observed phase pure LSF peaks in the goethite derived product, while hematite peaks were still observed in the product after heating mechanically activated mixture from hematite. The phase analysis together with other crystallographic parameters evaluated by Rietveld refinement is listed in Table 1.

For detailed identification of Fe phases formed during milling and annealing, ^{57}Fe Mössbauer spectroscopic analysis was used. Fig. 2 shows room temperature ^{57}Mössbauer spectra of both stoichiometric mixtures comprising Li_2O, SiO_2 and different Fe source, i.e., α Fe_2O_3 or 2α FeO(OH), milled for 60 min and subsequently isothermally treated at 1000 °C for 60 min. Mössbauer spectra of intact Fe sources are also shown for comparison. On both Mössbauer spectra after heating the

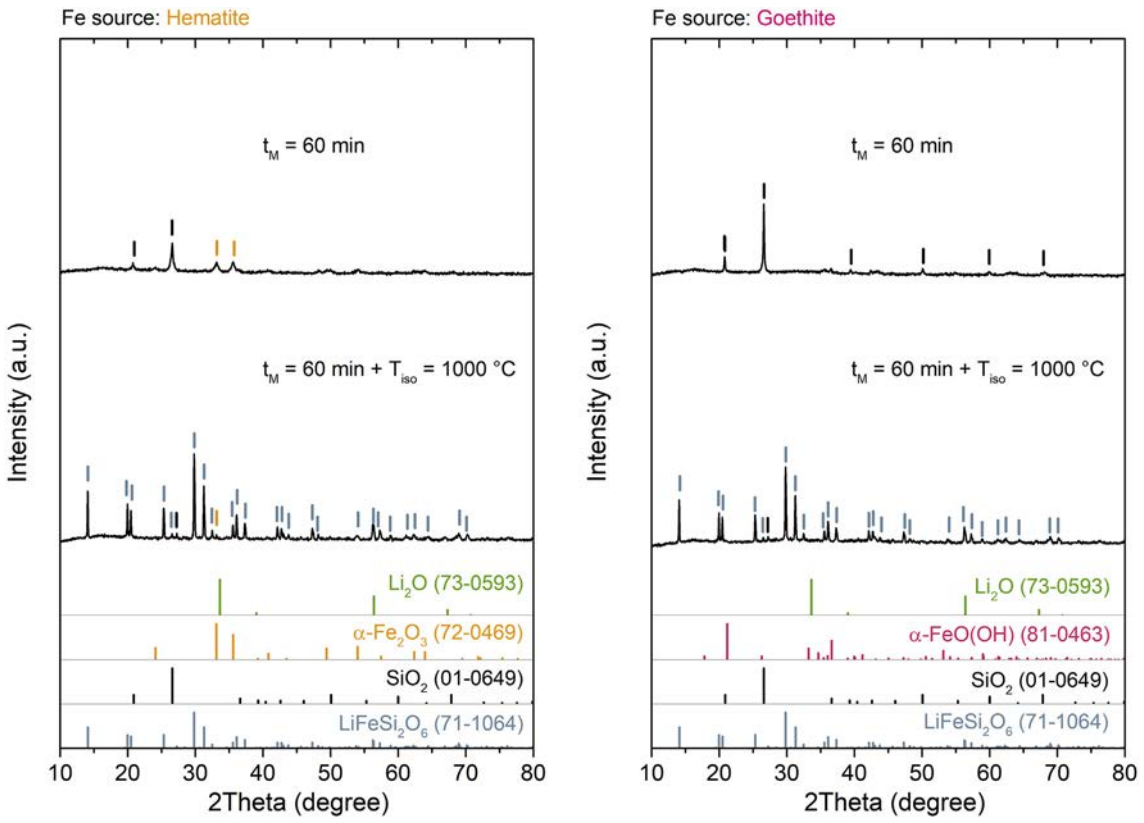

Fig. 1. XRD patterns of stoichiometric Li_2O + Fe_2O_3 + $4SiO_2$ (left) and Li_2O + 2FeO(OH) + $4SiO_2$ (right) mixtures after milling and thermal treatment. t_M = milling time.

milled mixture, a doublet was observed as a main spectral component, characteristic for Fe^{3+} ion in octahedral coordination. Its high sym metrical feature, together with the relatively small values of both the isomer shift (IS) and quadrupole splitting (QS), see Table 2, are in dicators of highly ordered octahedra, and hence, the high crystallinity of the product [19]. We note, that the spectrum is very similar to those reported by Zhou et al. for the sample prepared via a hydrothermal process and subsequent prolonged heating [20]. A closer observation reveals, however, a weak sextet, corresponding to the unreacted he matite (~5.5 at.%) in the product prepared from the mixture with he matite. These results are in line with the XRD profiles shown in Fig. 1. This confirms the superiority of goethite, as an iron source, for the solid state synthesis of phase pure LFS.

The difference in the reactivity of both mixtures during heating was studied by thermal analysis and infrared spectroscopy. As shown in Fig. 3a, TG/DTG DTA profiles of both 60 min mechanically activated mixtures with different Fe sources are entirely different, despite the close similarity of their FT IR spectra (compare orange and pink lines in Fig. 3b), except for significant difference in intensity of peak at 3460 cm^{-1}, characteristic for OH groups.

To interpret the difference in the obtained thermal profiles, the role of coexisting Li_2O should be referred, since it possesses high affinity to H_2O available from neighboring goethite. In the case of goethite alone (Fig. S2 bottom), the first DTG peak below 200 °C is simply interpreted as surface water desorption and the second DTG peak at around 270 °C is due to dehydrating decomposition to Fe_2O_3. The corresponding total weight losses observed were 7.9 mass% and 16.2 mass%, which are larger than the theoretical ones (4.04 mass% and 10.14 mass%) as well as larger than obtained in the reaction mixtures, respectively. The dif ference is ascribed to the adsorbed water. However, with the coexisting reaction partners, the relative intensity of the two DTG peaks is re versed. The larger weight loss peak at the lower temperature is due to the decomposition of goethite, which may be catalyzed by coexisting Li. Catalytic activity of Li containing species on the metal hydroxide de composition is well documented [21]. It is clear that easier decom position of goethite at lower temperatures eases availability of Fe^{3+}, necessary for the nucleation of $LiFeSi_2O_6$.

FTIR spectra of both mechanically activated mixtures before and after heating are displayed in Fig. 3b. The spectra after thermal analysis (green and blue lines) look almost identical for both cases, i.e. peak positions and intensities are characteristic for LFS. Thus, we may safely mention that the difference in the iron sources occurs at the early stage of heating after mechanical activation, as discussed above in conjunc tion with the thermal analyses.

Table 1
Phase analysis and crystallographic parameters evaluated by Rietveld analysis of the stoichiometric mixtures composed of Li_2O, SiO_2 and various Fe sources milled for 60 min and subsequently isothermally treated at 1000 °C for 60 min.

Fe source	Phase	a (Å)	b (Å)	c (Å)	Average crystallite size (nm)	Strain (10^{-4})	Fraction content (%)
Fe_2O_3	**α-Fe_2O_3**	5.0394(4)	5.0394(4)	13.7567(9)	–	–	2.1(5)
	SiO_2	4.9401(4)	4.9401(4)	5.3879(9)	–	–	2.4(4)
	$LiFeSi_2O_6$	9.6658(2)	8.6693(2)	5.2932(1)	239(3)	8.1(7)	95.5(9)
FeO(OH)	**SiO_2**	4.9143(9)	4.9143(9)	5.4644(9)	–	–	3.1(3)
	$LiFeSi_2O_6$	9.6708(2)	8.6696(3)	5.2933(4)	123(7)	4.6(1)	96.9(12)

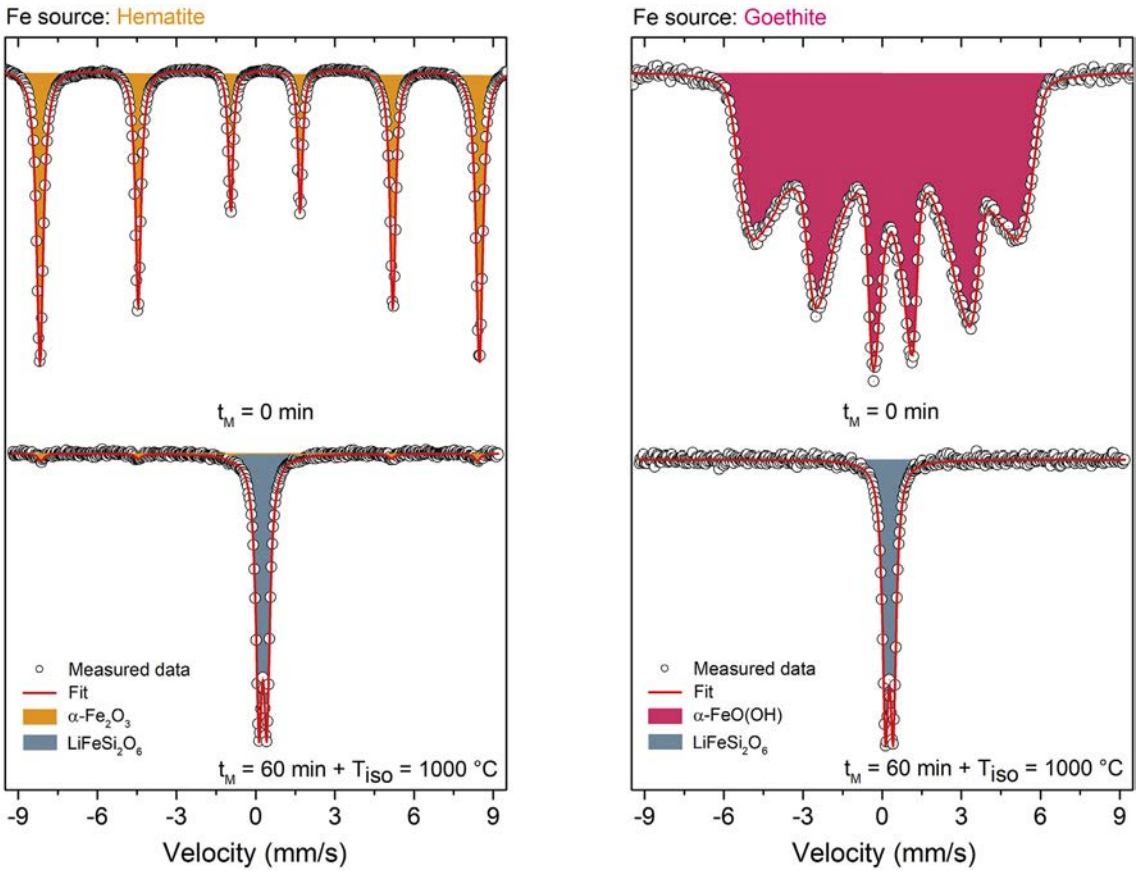

Fig. 2. Room-temperature ^{57}Fe Mössbauer spectra of stoichiometric Li_2O + Fe_2O_3 + $4SiO_2$ (left) and Li_2O + 2FeO(OH) + $4SiO_2$ (right) mixtures before/after milling and thermal treatment. t_M = milling time.

Table 2
Hyperfine parameters (IS: isomer shift, QS: quadrupole splitting, B_{hf}: magnetic hyperfine field, *I*: relative intensity of the spectral component) obtained by fitting the room-temperature ^{57}Fe Mössbauer spectra of the stoichiometric mixtures composed of Li_2O, SiO_2 and various Fe sources milled for 60 min and subsequently heated isothermally in air at 1000 °C for 60 min.

Fe source	Subspectrum	Phase	IS (mm/s)	QS (mm/s)	B_{hf} (T)	*I* (%)
α-Fe_2O_3	Sextet	α-Fe_2O_3	0.35(4)	0.21(8)	51.3(6)	5.5(0)
	Doublet	$LiFeSi_2O_6$	0.37(5)	0.29(9)	–	94.4(9)
α-FeO(OH)	Doublet	$LiFeSi_2O_6$	0.37(6)	0.29(4)	–	100.0

One of the most prominent effects of mechanical activation of the precursors is a preliminary charge transfer enabling the entire elec tronic states shift closer to that of the final product prior to heating [15]. Therefore, the effects of milling could be elucidated by the changes of electronical structure, examined by X ray photoelectron spectroscopy.

As shown in Fig. 4a, the Si2p peaks tally well with those reported for $LiAlSi_2O_6$ [22] and other pyroxenes [23]. Out of the two O1s peaks (Fig. 4b), the larger (O1s1) and smaller (O1s2) ones mainly reflect those of Si O and Fe(III) O, respectively [24]. Fe2p XPS profiles are shown in Fig. 4c. Between two well established Fe2p peaks, i.e., $2p_{3/2}$ at around 711 eV and $2p_{1/2}$ at around 724 eV, we observed less defined peaks at around 718 eV. The latter is often coined as a satellite peak, due to the electrons in partially filled d orbitals [25 27]. Although the satellite peak appears diffuse, we tried to separate it as a third peak. The changes in the binding energy (BE) by milling and subsequent heating are summarized in Table 3. The most significant differences between non treated and post heated products are observed in satellite peaks of Fe(III). The smaller change in BE generally implies that the electronic states of the activated mixture are closer to those of the post heated product, as it is in the case with goethite. From all these XPS observations, we may conclude that mechanical activation promotes the change in the electronic states of the reaction mixture toward those of the products. In addition, the mixture with goethite comes closer to that of the final product, just after milling, prior to heating. This may indicate preformation of the product nuclei at the temperature lower than that with hematite. These are the key issues of soft mechan ochemical processes, i.e. a combined mechanical/thermal process [15,28,29].

3.2. Physico chemical properties of the products, $LiFeSi_2O_6$

The phase purity of prepared $LiFeSi_2O_6$ was confirmed additionally by magnetic measurements. Temperature dependences of magnetic susceptibility, χ, and inverse susceptibility $1/\chi$ are shown in Fig. 5. The value of external magnetic field of 1 T was chosen due to comparative purpose with previous report [6]. The temperature dependences of magnetic susceptibility in zero field cooling (ZFC) and field cooling (FC) regimes clearly shows the peak at around 20 K (Fig. 5a). This is attributed to the phase transition to the antiferromagnetic ordered state [6]. This finding is in a good agreement with previous results, i.e. variation of T_N between 17.5 and 20.8 K [14,30]. We note, however,

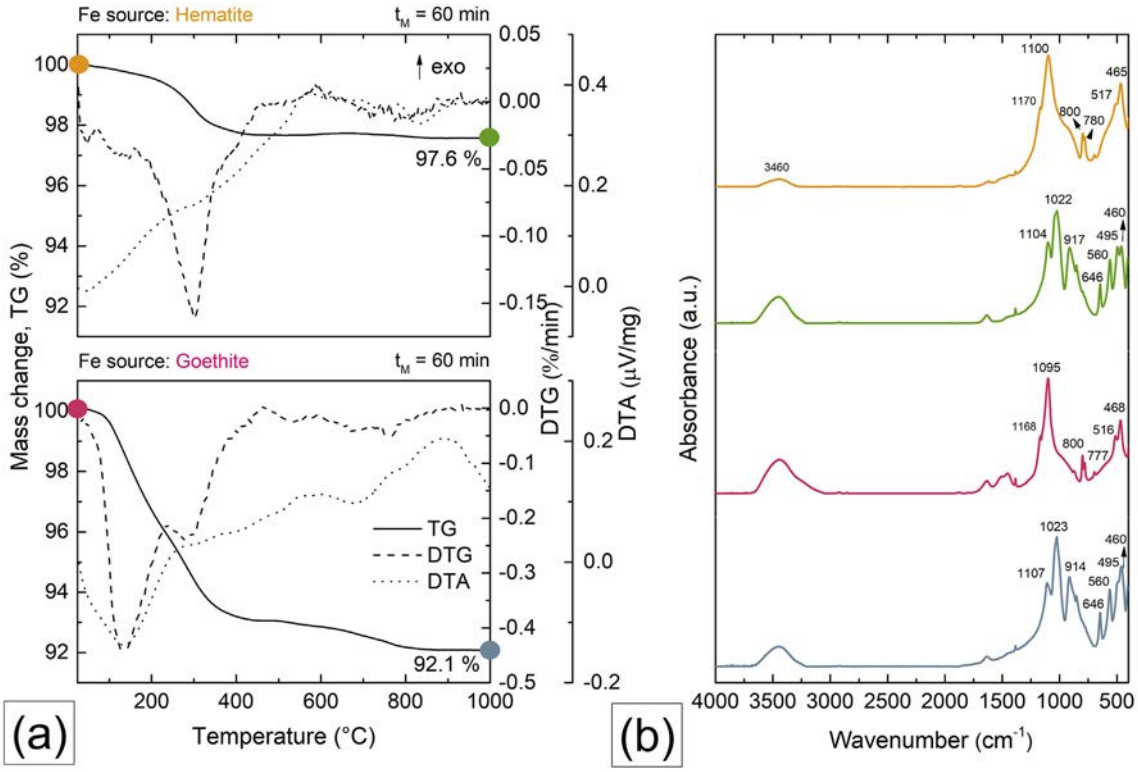

Fig. 3. (a) Thermal analysis (TG/DTG-DSC) conducted under air atmosphere of the stoichiometric $Li_2O + Fe_2O_3 + 4SiO_2$ (top) and $Li_2O + 2FeO(OH) + 4SiO_2$ (bottom) mixtures after milling (t_M = milling time). Colored markers indicate the samples at the point of thermal treatment characterized by FT-IR spectroscopy; (b) FT-IR spectra of mechanically activated mixtures before and after thermal process.

that the samples of the former were obtained by a solid state process by heating at 900° or 950 °C in polycrystalline form for more than one month [14], or even at T = 1300 °C under pressure P = 3 GPa provided single crystal [30] and the latter a natural mineral donated by the British Museum of Natural History. Our product contain a small amount of silica, as shown in Table 1, which does not influence its magnetic properties. Note that the samples prepared by Mauria et al. [14], referred as our reference, also contained silica in a small amount, very similar to ours.

The inverse susceptibility was analyzed in the frame of Curie Weiss law (Fig. 5b) in the temperature range from 70 K to 400 K. The analysis yielded the Curie constant C = 4.74 ± 0.05 emu K/mol which pro vides g factor, g = 2.076, and the Curie Weiss temperature Θ_{CW} = 33 ± 0.02 K. These results are in excellent agreement with the work by

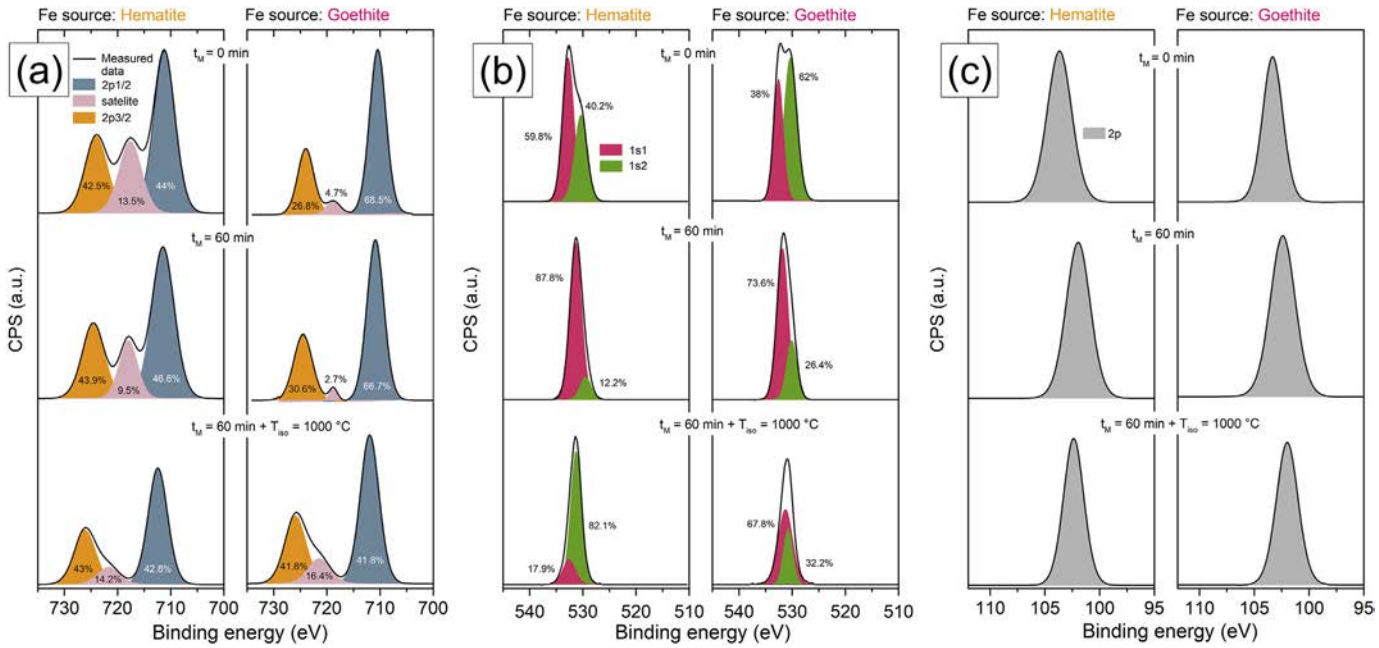

Fig. 4. (a) Fe2p, (b) O1s, (c) Si2p XPS spectra of stoichiometric $Li_2O + Fe_2O_3 + 4SiO_2$ (left) and $Li_2O + 2FeO(OH) + 4SiO_2$ (right) mixtures before/after milling and thermal treatment. t_M = milling time.

Table 3
Position of Fe2p, Si2p and O1s orbitals in stoichiometric $Li_2O + Fe_2O_3 + 4SiO_2$ and $Li_2O + 2FeO(OH) + 4SiO_2$ mixtures after three preparation stages: 1 – without treatment, 2 – after mechanical activation, 3 – after mechanical and thermal treatment.

Fe source	Preparation stage			Fe2p			O1s		Si2p
	Nr.	milling	heating	2p3/2	satellite	2p1/2	1s2	1s1	2p3/2
Fe_2O_3	1	–	–	711.20	717.59	723.99	530.38	532.79	103.67
	2	yes	–	711.45	717.96	724.55	529.48	531.33	101.97
	3	yes	yes	712.41	721.64	726.11	531.28	532.61	102.38
FeO(OH)	1	–	–	710.43	718.76	723.96	530.35	532.58	103.33
	2	yes	–	710.88	718.77	724.48	530.11	531.82	102.40
	3	yes	yes	711.95	721.43	725.90	530.79	531.29	101.96

Baum et al. [6]. The temperature dependence of the effective magnetic moment μ_{eff} calculated using the relation $\mu_{eff} = 2.83(\chi T)^{1/2}$ is shown in Fig. 6. The effective magnetic moment has a saturation tendency at highest temperatures and at $T = 400$ K μ_{eff} reaches 5.91 μ_B which is very close to the typical value of 6.14 μ_B for Fe^{3+} in a high spin state with g factor, $g = 2.076$.

As shown in Fig. 7, the goethite derived LFS particles exhibit high crystallinity with highly disordered surface layer with the thickness of 10 15 nm. This is another feature of the combined mechano/thermal solid state processes [15]. It is not possible to determine the shape of the crystals unambiguously because of overlapping one another, but they appear to have irregular morphology rather than a round one. Apparently, the diameter of crystals vary in the frame of tens of nan ometers and they are evidently agglomerated with random orientation into micrometric particle. Each of visible atomic planes families relate to different crystallographic orientations and hence indicate the pre sence of fine crystals. Areas of the same crystallographic orientations are selected by dashed lines and labelled with corresponding Miller indices. Individual FFT patterns, taken from these areas, are embedded. Reflections associated with a given plane system are indicated by the white arrow. Each pattern contains other reflections as well, which belongs to surrounding areas and could not be avoided when images were processed by Fourier transformation. The measured interplanar distances of systems 111, 211 and 321 with the average interplanar distance, $d_{(111)} = 0.2698$ nm, $d_{(211)} = 0.3567$ and $d_{(321)} = 0.204$ nm, fit to $LiFeSi_2O_6$ phase and are in accordance with the data stated in Table 1. It is very like that the two adjacent regions with the indicated orientation of planes 211, particularly the pair at the bottom of Fig. 7, create one crystal that only contains structural defects because their mutual misorientation is very small. These structural defects are usually induced by mechanical impact.

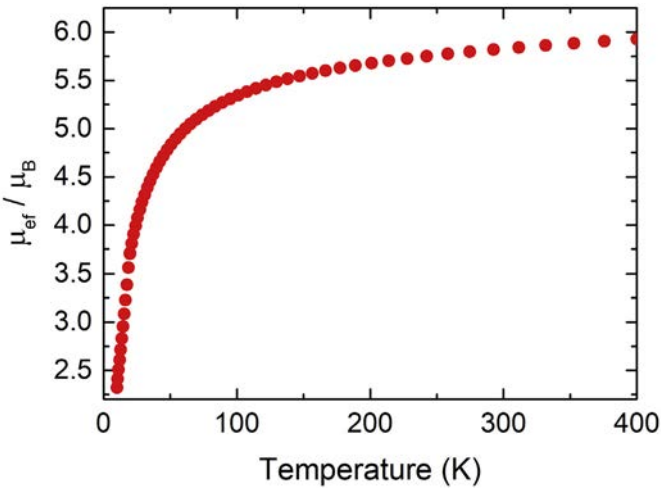

Fig. 6. Temperature dependence of the effective magnetic moment of $LiFeSi_2O_6$ prepared by mechano/thermal synthesis using α-FeO(OH) as Fe source.

3.3. Possible other differences in reactivity between goethite and hematite

In conjunction with the thermal analyses, superiority of goethite over hematite for phase pure synthesis was discusses by focusing on the coexistence of OH group. There are other viewpoints, e.g., hardness or deformability. The Mohs hardness of hematite is 6 7.5 and 5 5.5 for goethite. Softer materials tend to coat the harder ones during milling to form shell with the harder one as core [29,31]. This enables more in timate contact within the species in the precursor [32]. Furthermore, such intimate contact of dissimilar ingredients will increase in the nu cleation site leading to the smaller crystallite size, which was actually observed.

Hematite is anhydrous while goethite has polar OH group in its structure. As already mentioned with reference to Fig. 3a, thermal de composition not only donates H_2O, but also prone to incorporate hither amount of structural imperfections [28]. As a matter of fact, mechan ochemical transformation from goethite to hematite takes place during

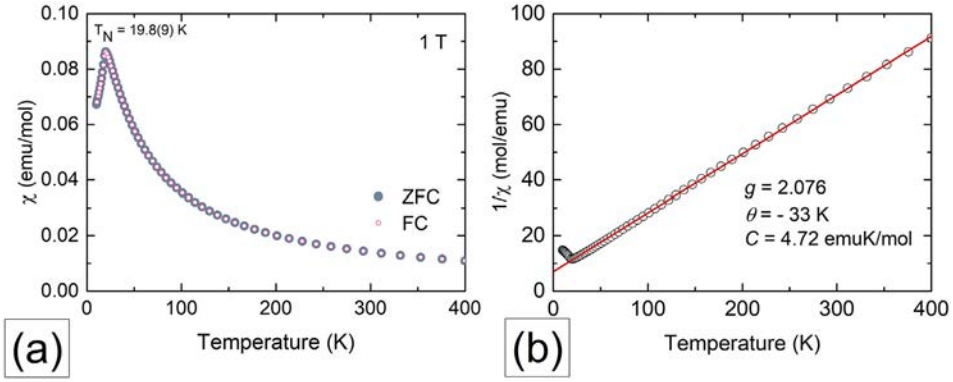

Fig. 5. (a) Temperature dependence of the magnetic susceptibility measured in ZFC (full circles) and FC (empty circles) regimes and (b) inverse susceptibility of $LiFeSi_2O_6$ prepared by mechano/thermal synthesis using α-FeO(OH) as Fe source and measured in an applied field of 1 T.

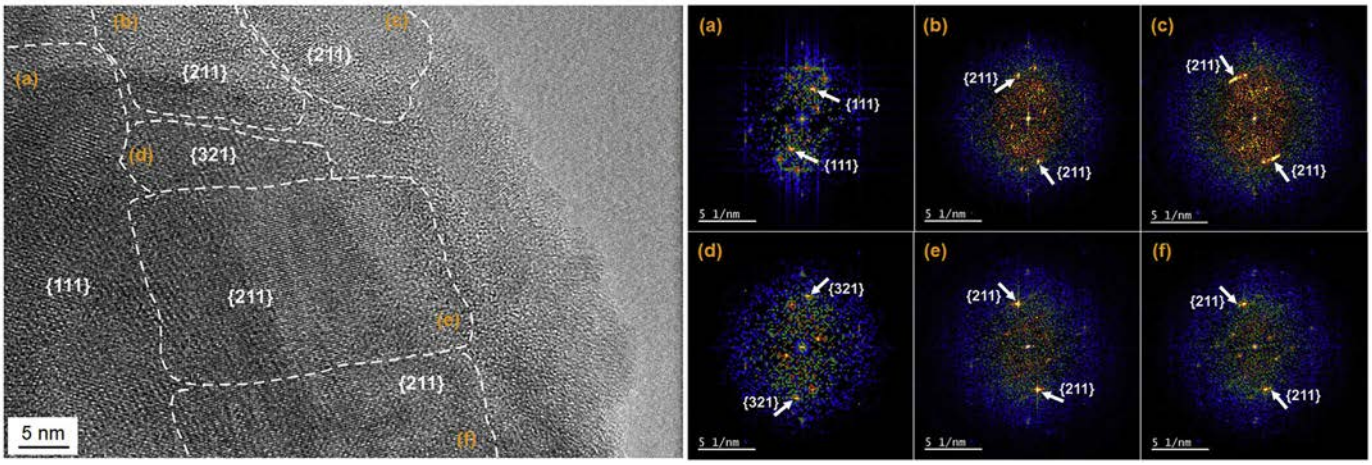

Fig. 7. TEM of $LiFeSi_2O_6$ prepared by mechano/thermal synthesis using α-FeO(OH) as Fe source and individual FFT patterns.

milling [33,34]. Related structural change, accompanied by dehydra tion during milling and heating, is associated with the extended concept of Hedvall effects [35,36].

4. Conclusions

By milling a stoichiometric mixture comprising α FeO(OH), Li_2O and SiO_2 by a planetary mill for 60 min and subsequent linear heating in air up to 1000 ˚C, the phase pure LFS ($LiFeSi_2O_6$) with ca 120 nm crystallites was obtained. This was superior over those prepared from hematite by the same procedure, with persistence of hematite, and a doubled crystallite size. Phase purity of the goethite derived LFS was also confirmed by Mössbauer spectroscopy, i.e. its spectrum comprises only a symmetrical doublet and free from a trace of a sextet sub spec trum typical for hematite. Magnetic properties of goethite derived LFS are very similar to those of the powders prepared by heating at 1173 1223 K for more than a month, or of a natural mineral. A higher reactivity of goethite leading to the phase pure LFS is primarily at tributed to the dehydration of goethite at the early stage of heating. This was confirmed by the thermal decomposition of hydroxides, ac celerated by Li_2O, as an additional factor of higher reactivity. The dif ference in the starting iron sources was also observed by XPS, indicating the electronic states of the mechanically activated mixture closer to the final products in case of the mixture with goethite. Easier plastic de formation, amorphization and phase transformation during the reaction may be additional items for the higher reactivity of goethite toward acquisition of phase pure LFS. Thus, the present combined mechano/ thermal preparative method is more sustainable than those of the conventional synthesis routes.

Declaration of competing interest

The authors declare that they have no known competing financial interests or personal relationships that could have appeared to influ ence the work reported in this paper.

Acknowledgements

The present work is supported by VEGA Grants No. 2/0103/20 and No. 2/0055/19 of the Scientific Grant Agency of the Ministry of Education, Science, Research and Sport of the Slovak Republic and the Slovak Academy of Sciences as well as by the Slovak Research and Development Agency (project APVV 14 0073). V.Š. acknowledges the support by the Deutsche Forschungsgemeinschaft (project SE 1407/4 2). This work was also performed within the frame of the project „Research Centre of Advanced Materials and Technologies for Recent and Future Applications „PROMATECH“, ITMS 26220220186, sup ported by the Operational Program “Research and Development” fi nanced through European Regional Development Fund.

References

[1] N. Morimoto, Nomenclature of pyroxenes, Mineral. Petrol. 39 (1988) 55–76.
[2] M. Cameron, J.J. Papike, Structural and chemical variations in pyroxenes, Am. Mineral. 66 (1981) 1–50.
[3] R.A. Howie, MINERALS | pyroxenes, in: Richard C. Selley, L. Robin M. Cocks, Ian R. Plimer (Eds.), Encyclopedia of Geology, Elsevier, 2005, pp. 567–569.
[4] E. Tóthova, R. Witte, M. Hegedűs, M. Senna, H. Hahn, P. Heitjans, V. Šepelák, Mechanochemical syntheses of $LiFeGe_2O_6$-based nanocomposite and novel na-noglassy $LiFeTi_2O_6$, J. Mater. Sci. 53 (2018) 13530–13537.
[5] J. Ni, Y. Kawabe, M. Morishita, M. Watada, N. Takeichi, T. Sakai, Pyroxene LiVSi2O6 as an electrode material for Li-ion batteries, J. Power Sources 195 (2010) 8322–8326.
[6] E. Baum, W. Treutmann, M. Behruzi, W. Lottermoser, G. Amthauer, Structural and magnetic properties of the clinopyroxenes NaFeSi2O6 and LiFeSi2O6, Z. Kristallogr. 183 (1988) 273–284.
[7] G.J. Redhammer, G. Roth, W. Paulus, G. Andre, W. Lottermoser, G. Amthauer, W. Treutmann, B. Koppelhuber-Bitschnau, The crystal and magnetic structure of Li-aegirine LiFe 3+ Si 2 O 6 : a temperature-dependent study, Phys. Chem. Miner. 28 (2001) 337–346.
[8] G.J. Redhammer, G. Roth, W. Treutmann, M. Hoelzel, W. Paulus, G. André, C. Pietzonka, G. Amthauer, The magnetic structure of clinopyroxene-type LiFeGe2O6 and revised data on multiferroic LiFeSi2O6, J. Solid State Chem. 182 (2009) 2374–2384.
[9] E. Turianicová, R. Witte, K.L. Da Silva, A. Zorkovská, M. Senna, H. Hahn, P. Heitjans, V. Šepelák, Combined mechanochemical/thermal synthesis of micro-crystalline pyroxene LiFeSi2O6 and one-step mechanosynthesis of nanoglassy LiFeSi2O6 based composite, J. Alloys Compd. 707 (2017) 310–314.
[10] S. Jodlauk, P. Becker, J.A. Mydosh, D.I. Khomskii, T. Lorenz, S.V. Streltsov, D.C. Hezel, L. Bohaty, Pyroxenes: a new class of multiferroics, J. Phys. Condens. Matter 19 (2007).
[11] S. Zhou, W.G. Zeier, M.C. Kemei, M.T. Sougrati, M. Mecklenburg, B.C. Melot, Hydrothermal preparation and magnetic properties of NaFeSi2O6: nanowires vs bulk samples, Inorg. Chem. 53 (2014) 12396–12401.
[12] N. Ishida, K. Sakatsume, N. Kitamura, Y. Idemoto, Improvement of electrochemical property of pyroxene-type LiFeSi2O6 and crystal-structure analysis, J. Ceram. Soc. Jpn. 125 (2017) 281–286.
[13] G.J. Redhammer, G. Tippelt, G. Roth, W. Lottermoser, G. Amthauer, Structure and Mossbauer spectroscopy of barbosalite Fe2+Fe23+ (PO4)(2)(OH)(2) between 80 K and 300 K, Phys. Chem. Miner. 27 (2000) 419–429.
[14] R.K. Maurya, P. Sharma, R. Rawat, R.S. Singh, R. Bindu, Structural response to the magnetic pre-ordering in LiFeSi2O6, Eur. Phys. J. B (2019) 92.
[15] M. Senna, A straight way toward phase pure complex oxides, J. Eur. Ceram. Soc. 25 (2005) 1977–1984.
[16] H. Kurokawa, M. Senna, Morphology control of goethite acicular particles during aging by nitrogen bubbling and subsequent reactive aeration, J. Mater. Sci. 43 (2008) 4737–4741.
[17] J. Rodriguez-Carvajal, Fullprof Program, (1993) Grenoble, France.

[18] J.C.o.P. Diffraction, Newtown Square, (2004) PA.
[19] W.A. Dollase, W.I. Gustafson, Fe-57 mossbauer spectral-analysis of the sodic clinopyroxenes, Am. Mineral. 67 (1982) 311–327.
[20] S.L. Zhou, G. King, D.O. Scanlon, M.T. Sougrati, B.C. Melot, Low temperature preparation and electrochemical properties of LiFeSi2O6, J. Electrochem. Soc. 161 (2014) A1642–A1647.
[21] A. Shkatulov, Y. Aristov, Modification of magnesium and calcium hydroxides with salts: an efficient way to advanced materials for storage of middle-temperature heat, Energy 85 (2015) 667–676.
[22] C.D. Wagner, D.E. Passoja, H.F. Hillery, T.G. Kinisky, H.A. Six, W.T. Jansen, J.A. Taylor, Auger and photoelectron line energy relationships in aluminum-oxygen and silicon-oxygen compounds, J. Vac. Sci. Technol. 21 (1982) 933–944.
[23] V.P. Zakaznova-Herzog, H.W. Nesbitt, G.M. Bancroft, J.S. Tse, Characterization of leached layers on olivine and pyroxenes using high-resolution XPS and density functional calculations, Geochem. Cosmochim. Acta 72 (2008) 69–86.
[24] V.P. Zakaznova-Herzog, H.W. Nesbitt, G.M. Bancroft, J.S. Tse, High resolution core and valence band XPS spectra of non-conductor pyroxenes, Surf. Sci. 600 (2006) 3175–3186.
[25] M.F. Descostes, N. Thromat, C. Beaucaire, M. Gautier-Soyer, Use of XPS in the determination of chemical environment and oxidation state of iron and sulfur samples: constitution of a data basis in binding energies for Fe and S reference compounds and applications to the evidence of surface species of an oxidized pyrite in a carbonate medium, Appl. Surf. Sci. 165 (2000) 288–302.
[26] C. Iacovita, R. Stiufiuc, T. Radu, A. Florea, G. Stiufiuc, A. Dutu, S. Mican, R. Tetean, C.M. Lucaciu, Polyethylene glycol-mediated synthesis of cubic iron oxide nanoparticles with high heating power, Nanoscale Res. Lett. 10 (2015) 391.
[27] S.J. Rajoba, L.D. Jadhav, P.S. Patil, D.K. Tyagi, S. Varma, B.N. Wani, Enhancement of electrical conductivity of LiFePO4 by controlled solution combustion synthesis, J. Electron. Mater. 46 (2016) 1683–1691.
[28] M. Senna, Grinding of mixture under mild condition for mechanochemical complexation, Int. J. Miner. Process. 44–5 (1996) 187–195.
[29] M. Senna, J. Pavlic, T. Rojac, B. Malic, M. Kosec, G. Brennecka, Preparation of phase-pure K0.5Na0.5NbO3Fine powders by a solid-state reaction at 625°C from a precursor comprising Nb2O5and K,Na acetates, J. Am. Ceram. Soc. 97 (2014) 413–419.
[30] R.G. Redhammer GJ, W. Paulus, G. Andre, W. Lottermoser, G. Amthauer, W. Treutmann, Koppelhuber-Botschmau, The crystal and magnetic structrure of Li-aegorome LiFe3 + Si2O6: a temperature-dependent study, Phys. Chem. Miner. 28 (2000) 337–346.
[31] T. Kinoshita, M. Senna, Y. Doshida, H. Kishi, Synthesis of size controlled phase pure KNbO3 fine particles via a solid-state route from a core–shell structured precursor, Ceram. Int. 38 (2012) 1897–1904.
[32] P. Balaz, M. Achimovicova, M. Balaz, P. Billik, Z. Cherkezova-Zheleva, J.M. Criado, F. Delogu, E. Dutkova, E. Gaffet, F.J. Gotor, R. Kumar, I. Mitov, T. Rojac, M. Senna, A. Streletskii, K. Wieczorek-Ciurowa, Hallmarks of mechanochemistry: from nanoparticles to technology, Chem. Soc. Rev. 42 (2013) 7571–7637.
[33] Y. Cudennec, A. Lecerf, Topotactic transformations of goethite and lepidocrocite into hematite and maghemite, Solid State Sci. 7 (2005) 520–529.
[34] L.A. Perez-Maqueda, J. Subrt, V. Balek, J.M. Criado, C. Real, Use of emanation thermal analysis in characterisation of nanosized hematite prepared by dry grinding of goethite, J. Therm. Anal. Calorim. 60 (2000) 997–1007.
[35] A.S. Bliznakov G, S. Manev, The Hedvall effect in the decomposition of hydrogen peroxide on single crystals of a-Cr2O3, J. Catal. 33 (1974) 138–141.
[36] S.J. Gallagher Pk, P.M. Woodward, I.N. Lokuhewa, Reactions within the system 2SrCO3–Fe2O3, Part I. CO2 atmosphere, J. Therm. Anal. Calorim. 80 (2005) 217–223.